Advances in Biological Regulation 89 (2023) 100976

Contents lists available at ScienceDirect

Advances in Biological Regulation

journal homepage: www.elsevier.com/locate/jbior

A possible role for G-quadruplexes formation and DNA methylation at *IMOOD* gene promoter in Obsessive Compulsive Disorder

Annalaura Sabatucci [a,1], Antonio Girella [a,1], Martina Di Bartolomeo [a], Mariangela Pucci [a,b], Matteo Vismara [c], Beatrice Benatti [c], Isobel Alice Blacksell [d], Dianne Cooper [d], Enrico Dainese [a], Fulvio D'Acquisto [d,e], Bernardo Dell'Osso [c,f,**], Claudio D'Addario [a,g,*]

[a] *Department of Bioscience and Technology for Food, Agriculture and Environment, University of Teramo, Teramo, Italy*
[b] *Department of Biosciences and Nutrition, Karolinska Institute, Huddinge, Sweden*
[c] *Department of Biomedical and Clinical Sciences Luigi Sacco, University of Milan, Milano, Italy*
[d] *William Harvey Research Institute, Barts and The London School of Medicine and Dentistry, Queen Mary University of London, London, UK*
[e] *School of Life and Health Science, University of Roehampton, London, SW15, 4JD, UK*
[f] *Department of Biomedical and Clinical Sciences "Luigi Sacco", Psychiatry Unit 2, ASST Sacco-Fatebenefratelli, Via G.B. Grassi, 74, 20157, Milan, Italy*
[g] *Department of Clinical Neuroscience, Karolinska Institutet, Stockholm, Sweden*

ARTICLE INFO

Keywords:
OCD molecular markers
IMOOD
DNA methylation
G-quadruplex

ABSTRACT

Obsessive Compulsive Disorder (OCD) is a mental health condition still classified and diagnosed with subjective interview-based assessments and which molecular clues have not completely been elucidated. We have recently identified a new regulator of anxiety and OCD-like behavior called Immuno-moodulin (IMOOD) and, here, we report that *IMOOD* gene promoter is differentially methylated in OCD subjects when compared to genomic material collected from healthy controls and this alteration is significantly correlated with the increased expression of the gene in OCD. We also demonstrated that *IMOOD* promoter can form G-quadruplexes and we suggest that, in homeostatic conditions, these structures could evoke DNA-methylation silencing the gene, whereas in pathological conditions, like OCD, could induce gene expression making the promoter more accessible to transcriptional factors. We here thus further suggest *IMOOD* as a new biomarker for OCD and also hypothesize new mechanisms of gene regulation.

1. Introduction

In transgenic mice overexpressing Annexin-A1 specifically in T cells showing high level of compulsive repetitive digging and increased level of anxiety-like behavior, it was recently reported an overexpression of the gene coding for the Testis Development

* Corresponding author. Department of Bioscience and Technology for Food, Agriculture and Environment, University of Teramo, Teramo, Italy.
** Corresponding author. Department of Biomedical and Clinical Sciences Luigi Sacco, University of Milan, Milano, Italy.
E-mail addresses: bernardo.dellosso@unimi.it (B. Dell'Osso), cdaddario@unite.it (C. D'Addario).
[1] Equally contributing authors.

https://doi.org/10.1016/j.jbior.2023.100976
Received 5 August 2023; Accepted 7 August 2023
Available online 8 August 2023

Related Protein (*TDRP*) that we alternatively named Immuno-*mood*ulin (*IMOOD*) because of its discovery in T cells and ability to modulate anxiety-like behavior in mice (Piras et al., 2020), and from now on in the manuscript this is how we will refer to.

Of interest, the analysis of *IMOOD* mRNA levels in PBMCs of patients with Obsessive Compulsive Disorder (OCD) revealed a sixfold increase in gene expression when compared to healthy controls (Piras et al., 2020). These findings suggest IMOOD as the first blood protein biomarker of OCD and related behaviors and opens up to in-depth analysis of the molecular mechanisms by which *IMOOD* gene is regulated and overexpressed in OCD. Focusing on the study of this gene, the overall objective of this work is thus to suggest new tools to diagnose and stratify patients for their increased risk of developing OCD, a psychiatric condition responsible for a significant impairment of daily functioning and reduction in quality of life, for both patients and their caregivers (American Psychiatric Association, 2013; Dell'Osso et al., 2007; Fontenelle et al., 2010). Available treatments for OCD are yet partially effective (Koran and Simpson, 2013) with only one-third of people seeking for help (García-Soriano et al., 2014; Levy et al., 2013). Moreover, OCD patients might present themselves in a relatively healthy way when compared to subjects with other psychiatric conditions, and diagnostic criteria might not help detecting subjects with subthreshold symptoms (De Bruijn et al., 2010).

Thus far, very little is known on *IMOOD* gene and promoter regulation. Human *IMOOD* (Ensembl gene ENSG00000180190, Uniprot identifier Q86YL5) is a protein that was originally thought to contribute to normal sperm motility, but was later found not essential for male fertility. Recent works suggest that IMOOD could play a regulatory role not only in OCD but also in other psychiatric, neurodegenerative and/or autoimmune diseases. By Next Generation Sequencing (NGS), a mutation in *IMOOD* (chr8:442616;A4G) has been observed only in the affected twin from a pair of monozygotic twins discordant for gender dysphoria (Morimoto et al., 2017). GWAS and DNA sequencing data show a significant Single Nucleotide Polymorphism (SNP) associated with longevity in dogs and located in the 3′UTR of the *IMOOD* gene (Korec et al., 2022). 3′ Untranslated regions might have a relevant role in the regulation of translation and mRNA stability (Kuersten and Goodwin, 2003) and 3′UTR SNPs have been already described in humans associated with longevity (Crocco et al., 2016).

Moreover, a microduplication in band p23.3 of chromosome 8 was found to segregate with a broad spectrum of psychiatric problems and, of note, a significant association was observed for *FBXO25* and IMOOD, localized in the proximal part of the microduplication (Harich et al., 2020). When the authors were tempted to validate the relevance of their finding in Drosophila, they found two orthologues for *FBXO25*, whereas there aren't orthologues for *IMOOD*. As Drosophila does not have an adaptive immune system, it is possible to speculate that indeed *IMOOD* might be a genuine 'peripheral' modulator of anxiety behavior that is expressed in T cells. The hypothesis is also corroborated by the fact that *IMOOD* is not expressed in any invertebrate lacking an adaptive immune system.

The main goal of this work is to elucidate the role of *IMOOD* in the pathophysiology of OCD and better characterize its gene structure and regulation.

2. Methods and materials

2.1. Subjects

A total of 31 patients (21 women and 10 men; age: 38.19 ± 13.11) followed up at the OCD tertiary outpatient Clinic of the University Department of Psychiatry of Milan, Luigi Sacco Hospital were included in the study. Diagnoses were assessed by the administration of a semi-structured interview based on DSM-5 criteria (SCID 5 research version, RV) (First et al., 2015). In case of psychiatric

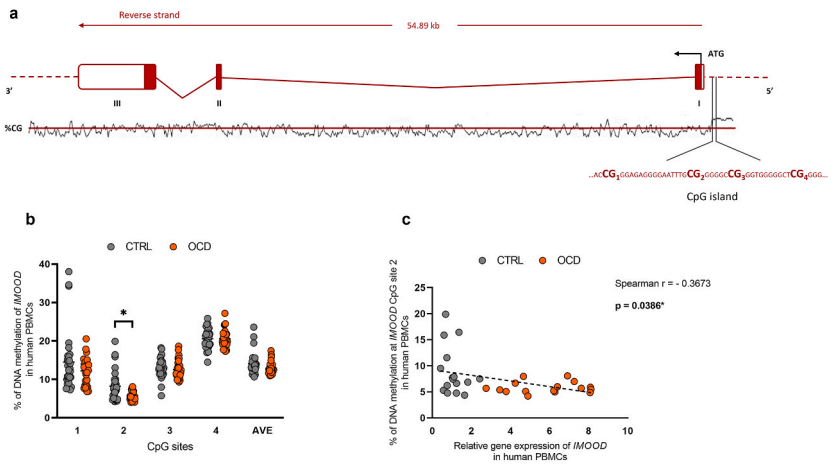

Fig. 1. a. Schematic representation of human IMOOD gene. Translation start codon (ATG), exons and introns are depicted. Coding regions of exons are shown filled. Sequence of the CpG island under study is also reported. Bold text indicates the 4 CpG sites analyzed; **b**. Percentage of DNA methylation of IMOOD promoter in human PBMCs from CTRL group vs. OCD. Focus on CpG sites 1,2,3,4 in CpG island located in Chr 8: 546,051–545,318. No interesting difference emerges from average values. A remarkable difference for CpG site 2 (*). **c**. Correlation between IMOOD gene expression and % change of DNA methylation at CpG site 2 of the same gene. Data were compared by Spearman's rank correlation coefficient. Spearman r and p value are shown.

comorbidity, OCD had to be the primary disorder and illness severity was measured through the Yale-Brown Obsessive Compulsive Scale (Y-BOCS) (Goodman et al., 1989). Presence of medical condition and/or drug abuse represented exclusion criteria. All patients were for at least one month on stable pharmacological treatment chosen according to international guidelines in the field (Koran and Simpson, 2013). A total of 30 age and sex-matched controls (18 women and 12 men; age: 36.70 ± 13.15) were volunteers without any psychiatric disorder, as determined by the nonpatient edition of the SCID and no positive family history for major psychiatric disorders in the first-degree relatives (Maxwell and Maxwell, 2013). All subjects had given their written informed consent to participate in the study, which included the use of personal and clinical data as well as blood drawing for genotyping and methylation analysis. The study protocol had been previously approved by the local Ethics Committee.

2.2. Analysis of IMOOD DNA methylation

To analyze methylation levels of *IMOOD*, Genomic DNA was isolated from human PBMCs, as previously described (Pucci et al., 2019).

500 ng of each purified DNA sample was subjected to bisulfite modification using the EZ DNA Methylation-Gold™ Kit (Zymo Research, Orange, CA, USA), inducing chemical conversion of unmethylated cytosine residues to uracil as previously described (D'Addario et al., 2019). The DNA methylation status of 4 CpG sites present in the *IMOOD* CpG island at gene promoter, predicted through MethPrimer (Li and Dahiya, 2002), was assessed using a pyrosequencing assay.

The schematic representation of the CpG island under study at *IMOOD* human gene is shown in Fig. 1a, whereas the exact locations of the CpG sites analyzed are reported in Table 1.

CpG methylation assay was designed through PyroMark Assay Design Software 2.0 (Qiagen, Hilden, Germany). We chose to analyze the sequence with the best score within a CpG island spanning from 8:545,322 to 8:546,094. PCR and Sequencing primers and the related assay score are reported in Table 2.

DNA, after bisulfite treatment, was first amplified by PyroMark PCR Kit (Qiagen, Hilden, Germany) with a biotin labeled primer according to the manufacturer's recommendations. PCR conditions were as follows: 95 °C for 15 min, followed by 45 cycles of 94 °C for 30 s, 56 °C for 30 s, 72 °C for 30 s, and, finally, 72 °C for 10 min. Specificity of PCR products was then verified by electrophoresis. The sequencing was performed on a PyroMark Q48 Autoprep using Pyro Mark Q48 Advanced Reagents (Qiagen, Hilden, Germany), following the manufacturer's recommendations. DNA methylation level was analyzed through the PyroMark Q48 Autoprep 2.4.2 software which calculates the methylation percentage mC/ (mC + C) (mC = methylated cytosine, C = unmethylated cytosine) for each CpG site, allowing quantitative comparisons. Quantitative methylation results were expressed both as a percentage of every single CpG site and as the average of the methylation percentage of all the 4 CpG sites under study.

2.3. Bioinformatics

Pattern-based prediction of Transcription Factor Binding sites was performed using the Alggen promo database (Farré et al., 2003; Messeguer et al., 2002), setting a dissimilarity margin less or equal than 15%. Search for G4s was performed with the web-based server QGRS Mapper (Kikin et al., 2006), where the algorithm for the search of G4s scans the input sequence for the following motif: Gx - Ny1 - Gx - Ny2 - Gx - Ny3 - Gx, where x ≥ 2 is the number of G quartet stacks; y1,y2,y3 is the length of each loop between G groups, of arbitrary length. For our analysis, we set the parameters as follows: max length 45; minimum G-group size 2; loop size: 0–36.

2.4. AlphaScreen® assay

We performed an Alpha (Amplified Luminescence Proximity Homogeneous Assay) assay to test the ability of G4-forming oligos to bind to an anti-G4 monoclonal antibody (Biffi et al., 2013) before and after CpG methylation. This Ab has been shown to bind G4 structures with different symmetries *in vitro* by ELISA and in immunocytochemistry experiments (Biffi et al., 2013), and it has been successfully utilized in ChIP-seq experiments (Hänsel-Hertsch et al., 2016).

The following oligonucleotides were purchased from IDT (www.idtdna.com)

b*IMOOD*	5' – b- GAG AGG GGA ATT TGC GGG GGC CGG GTG GGG GCT CGG GGG – 3′
IMOOD	5' – GAG AGG GGA ATT TGC GGG GGC CGG GTG GGG GCT CGG GGG – 3′
b*KIT2*	5′– b- AGA CCC GGG CGG GCG CGA GGG AGG GT – 3′
KIT2	5' – CGG GCG GGC GCG AGG GAG GGT – 3′
*KIT2*mut	5′– CTT TCT TTC GCG ATT TAT TTT – 3′
b2stackg4	5′– b-GGA GGT ATC ATA TGA CAG TGA ACT TCA AGG AAC TAT GGA ACC CTC TTA TGG ACT CCC – 3′

Table 1
Location of the CpG sites under study at the human IMOOD gene. Genome assembly GRCh38: CM000670.2, transcript TDRP-201 (ENST00000324079.11).

Human *IMOOD* CpG Island (chromosome 8)			
CpG Site 1	CpG Site 2	CpG Site 3	CpG Site 4
8: 545,398	8: 545,381	8: 545,374	8: 545,362

Table 2
Primer set used for CpG methylation assay.

Primer Set[a]			Score: 89 Quality: High		
Primer	Id	Sequence	Nt	Tm, °C	%GC
→ PCR	F1	GGGGGTAGTTAGGGAGTAAGTG	22	59.3	54.5
←+ PCR	R1	CTATCCCCCATTCCCTAAATCCTCCTCTA	29	60.1	48.3
→ Sequencing	S1	GGGGAGAAGGAGAGA	15	48.3	60.0
Sequence to Analyze	ATYGGGAGAG GGGAATTTGY GGGGGTYGGG TGGGGGTTYG GGGGTAGAGG AGGATTTAGG GAAT				

[a] Primers' characteristics like nucleotide number (**Nt**), melting temperature (**Tm, °C**) and percentage in GC (**%GC**) are reported. Reverse biotinylated primer is indicated (+). Analyzed sequence (after bisulfite conversion) and CpG methylation assay score are reported as well.

Anti-DNA G-quadruplex structures, clone BG4 Monoclonal Antibody (AbG4) was purchased at Merk Sigma-Aldrich. The AlphaScreen® FLAG (M2) no-wash assay kit containing Streptavidin Donor beads and Anti-FLAG conjugated AlphaScreen® Acceptor beads was purchased at PerkinElmer.

Biotinylated oligos were designed to bind to the assay kit streptavidin-tagged donor beads. The Acceptor beads are functionalized with an anti-FLAG antibody, able to bind to the FLAG-tag present in AbG4.

Alpha measurements were performed on an EnSpire Microplate Reader (PerkinElmer) using a standard Alpha method protocol for low volume 384 well plates. We utilized white Proxyplate-384 Plus, white shallow well microplates (PerkinElmer).

The following buffers were used to dissolve samples: Buffer A (Tris 10 mM pH 7.4, KCl 100 mM, Tween20 0.1% v/v); Buffer B (Tris 10 mM pH 7.4, KCl 100 mM, Tween20 0.1% v/v, BSA 1 mg/ml); Buffer C (Tris 10 mM pH 7.4 KCl 100 mM); Buffer D (Tris 10 mM pH 7.4).

In each microplate well we added 3 μl competitor in buffer A and 3 μl AbG4 30 nM in buffer B, then incubated 1 h in the dark at room T. Therefore, we added 3 μl b-oligo 30 nM in buffer A and 6 μl of a donor/acceptor mix beads in buffer B, and we read the Alpha signal after 2 h incubation in the dark at room T.

Before proceeding with the Alpha assay, all oligonucleotides were diluted at 15 μM in buffer A or buffer C and followed an annealing step. Annealing conditions were as follows: 95 °C for 5 min followed by a slow-cooling step (−0.05 °C/s) until reaching 21 °C to promote G4 structures formation.

2.5. Oligonucleotide methylation

Reagents for oligonucleotide methylation are from New England Biolabs. Methylation of *KIT2* and *IMOOD* oligos was performed according to producer recommended protocols. In Brief: 2 μl SAM 1.6 mM were incubated for 1 h at T = 37 °C with 1 μl of oligo (1 μg/μl), 1 μl Sssl methylase (4U/μl), 2 μl NEB buffer and 14 μl nuclease-free water. The reaction was stopped by heating samples at 65 °C for 20 min.

2.6. UV differential optical absorption spectroscopy

UV spectra in the 220–350 nm wavelength range, with a 1 nm step were measured using a nanodrop 2000C instrument (Thermo Scientific).

b*KIT*, *KIT*, *KIT*mut, b*IMOOD* and I*MOOD* oligonucleotides were diluted at 15 μM in buffer A, C, or D (same buffer compositions as in Alpha assays). Samples in buffer A and C were measured before and after an annealing step. Differential spectra were calculated on those normalized at the wavelength of 260 nm.

2.7. Statistical analysis

Statistical Data Analysis was performed using Prism® 9 (GraphPad Software, San Diego, CA). DNA methylation results at *IMOOD* promoter in OCD human samples are expressed as mean ± standard deviation (SD). DNA methylation at each CpG site was analyzed using the Mann-Whitney test and Sidak-Bonferroni correction was used for the multiple comparisons. Power calculations were performed using G*Power version 3.1 (Faul et al., 2007). All the data were compared by Spearman's rank correlation coefficient. P-values <0.05 were statistically significant. For Alpha assays, data points are reported as mean ± standard deviation (SD) of a triplicate. Experimental points were analyzed using a log(inhibitor) vs. response – Variable slope (four parameters) Least squares fit (Sabatucci et al., 2020).

3. Results

3.1. IMOOD promoter is differentially methylated in OCD patients

A significant decrease in *IMOOD* DNA methylation at gene promoter in OCD subject at CpG site 2 (CTRL: 8.22 ± 3.85; OCD: 5.78 ± 1.20; $p = 0.032$) was observed (Fig. 1b). Achieved Power was 0.91 for DNA methylation at this CpG site. Consistently, we also report an

inverse significant correlation between the already reported *IMOOD* gene expression (2^(−DDCt) values) (Piras et al., 2020) and DNA methylation at the same CpG 2 (Spearman's r = - 0.37, p = 0.038) (Fig. 1c). No significant correlations were observed when stratifying data according to age, gender, years of onset or Yale-Brown Obsessive Compulsive Scale (Y-BOCS) scores, a scale designed to measure the severity and type of OCD symptoms (see Supplementary Fig. S1).

3.2. IMOOD is predicted to contain G-quadruplexes

We performed a bioinformatic analysis of the CpG island of *IMOOD* promoter containing the CpG site resulted differentially methylated between OCD and controls, in search of possible Transcriptional Factors (TFs) binding sites that could promote/repress the transcription of this gene.

In this way, we identified, among the others, the presence of a potential consensus site for WT1, a complex zinc finger transcription factor that has been shown to activate or repress numerous target genes and to be sensitive to CpG methylation (Hashimoto et al., 2014).

Moreover, we noticed that the region contains 51 guanines, accounting for 55.4% of total nucleotides, that might predict for the formation of a G4 structure, a secondary DNA structure alternative to the double helix, which is observed upon stacking of typically 3 or more G-quartets, where a G quartet is a square planar structure formed by 4 guanine residues. We thus performed a bioinformatic prediction for the possible formation of G4s using QGRS mapper on the *IMOOD* promoter CpG island.

For this analysis, we also used as a positive control the promoter sequence of the proto-oncogen gene *KIT*, which contains 3 different and well-characterized G4 structures, namely *KIT1*, *KIT2* and *SP1* (Ducani et al., 2019) (GrCH38.p13 chromosome 4:54,657,830 - 54,657,906). As a negative control, we designed an oligo of the length of *KIT2* (21 nts), containing no guanines (*KIT2*mut). Finally, we also tested the program on a 54 nt synthetic sequence containing a possible 2-fold stack G4 (2stack G4). Results are reported in Table 3.

As expected, QGRS reported no results for *KIT2*mut oligo, addressing to zero the probability to form G4 structures, and a very low score for the synthetic oligo sequence, indicating a low probability of forming a 2-stack quadruplex, characterized by a very long connecting loop (23 nts).

In our positive control sequence *KIT*, the program returned 3 regions, corresponding respectively to the well-known G4 motifs *KIT2*, *SP1* and *KIT1*.

Regarding the *IMOOD* gene promoter oligo, 3 different regions are predicted to form G4s. Among them, the 35 nt-long 4-stack G4 in position 30 containing the observed differentially methylated CpG site resulted with at G-score of 106, much higher than the one calculated for the 3 G4 motifs in *KIT*.

Of note, expanding our analysis to the whole promoter, we observed that the considered CpG island belongs to a region, extending 761 nts from the tss in the 5' flanking tract containing 50% G.

In this region, QGRS predicted 17 different possible G4 non overlapping sequences. Among them, 5 with scores higher than 100 (the considered one being the 3rd best ranking) (data not shown).

3.3. Alpha assay: IMOOD forms G4 at promoter region

We verified *in vitro* the formation of the G4 structure predicted with the highest score at *IMOOD* promoter (*Imood*-B, see Table 3) setting up an Alpha assay based on the ELISA method proposed by Biffi and coll. (Biffi et al., 2013).

As a positive control for this method, we chose the *KIT2* sequence (see Table 3), already tested for AbG4 affinity (Biffi et al., 2013). Moreover, its 3-stack structure has been resolved by NMR in different conditions (Peterková et al., 2021).

After verifying that the buffer composition does not affect the Alpha measurements, by registering the Alpha signal of a biotinylated-FLAG standard sample at different concentrations in buffer B and in standard Alpha buffer, we optimized sample concentrations and incubation time (data not shown).

We then performed a competitive binding assay for measuring the affinity of G4-forming oligos vs AbG4 Ab. At fixed concentration

Table 3
QGRS Mapper G4 prediction results (overlaps not included).

Oligo[a]	POSITION	LENGTH	QGRS	G-score
IMOOD-A	2	14	GGCGGGGGAGAAGG	33
IMOOD-B	30	35	GGGGAATTTGCGGGGGCCGGGTGGGGGCTCGGGGG	106
IMOOD-C	69	19	GGAGGACCCAGGGAACCGG	32
KIT (KIT1)	7	20	GGGCGGGCGCGAGGGAGGGG	68
KIT (SP1)	28	17	GGCGAGGAGGGGCGTGG	36
KIT (KIT2)	57	21	GGGAGGGCGCTGGGAGGAGGG	69
KITmut	–	–		–
2stackG4	1	38	GGAGGTATCATATGACAGTGAACTTCAAGGAACTATGG	14

[a] Input sequences:IMOOD:CGG CGG GGG AGA AGG AGA GAA CCG GGA GAG GGG AAT TTG CGG GGG CCG GGT GGG GGC TCG GGG GTA GAG GAG GAC CCA GGG AAC CGG GGA TAKIT:AGA CCC GGG CGG GCG CGA GGG AGG GGA GGC GAG GAG GGG CGT GGC CGG CGC GCA GAG GGA GGG CGC TGG GAG GAG GGG KITmut:CTT TCT TTC GCG ATT TAT TTT 2stack G4:GGA GGT ATC ATA TGA CAG TGA ACT TCA AGG AAC TAT GGA ACC CTC TTA TGG ACT CCC.

of biotinylated oligos and AbG4 (30 nM) we added 7 points of a 1:3 serial dilution of 300 nM competitors. b*KIT2* competitors used are respectively *KIT2*, *KIT2* after methylation, *KIT2*mut; b*IMOOD* competitors: *IMOOD*, *IMOOD* methylated, *KIT2*mut. Data fitting parameters are reported in Table 4, experimental points and curves in Fig. 2.

Our results show how b*KIT2* has a good affinity vs AbG4, with a K_d of 337 nM. CpG methylation seems to slightly stabilize the structure, with a K_d value of 226 nM (see Fig. 2. This result is in line with what reported by Laddachote and coll (Laddachote et al., 2021). who showed that CpG methylation does not affect the structure and thermal stability of *KIT2* in the presence of K^+ ions in solution. The mutated sequence (*KIT2*mut) is substantially non-competitive, with a predicted K_d value of 15 μM (Fig. 2a).

IMOOD has higher affinity vs AbG4 ($K_d = 259$ nM) with respect to *KIT2*. Again, for this structure, CpG methylation has no structural destabilizing effect as the affinity vs AbG4 ($K_d = 274$ nM) remains unchanged within the error (Fig. 2b).

Interestingly, the 2stackG4 oligo, predicted to form G4s with low score, gave rise to a strong Alpha signal. A displacement assay, using *IMOOD* oligo as a competitor, allowed us to determine that this structure has anyway lower affinity vs AbG4, with a very low IC50 concentration (10 nM) (Fig. 2c).

3.4. UV differential absorbance spectroscopy confirms G4 formation and stability

The possible structural effects of the experimental conditions used in the Alpha assay (biotinylation, K^+ concentration, annealing step, addition of detergent in solution) on the observed G4 formation and stability have been thus analyzed by UV differential absorption spectroscopy. UV absorbance spectroscopy is a method largely used to assess the formation of G4 structures in solution. Upon G4 formation, a differential UV spectrum gives rise to characteristic peaks (Gray and Chaires, 2012; Karsisiotis et al., 2011).

We registered the absorption spectra of biotinylated and non-biotinylated oligonucleotides in buffer A and buffer C (before and after annealing) and calculated the differential spectra with respect to buffer D (Fig. 3).

The analysis of the differential spectra shows how the G4-forming oligonucleotides *KIT2* and *IMOOD* have typical differential spectra (Karsisiotis et al., 2011) with maxima around 244 and 276 nm, and minima around 260 and 290 nm while the mutated oligonucleotide *KIT2*mut, not competent for forming G4s, maintains the same conformation in all considered buffer compositions, and it is not influenced by the presence of K^+ ions in solution.

Biotinylation at the 5′-end of *KIT2* and *IMOOD* oligonucleotides seems to slightly influence G4 stability, as for these samples maxima and minima are less pronounced with respect to non-biotinylated ones.

KIT2 and b*KIT2* show an increase of the maximum at 244 ± 1 nm after annealing, addressing a possible G4 stabilization or symmetry variation. In the case of *IMOOD* and b*IMOOD*, the differential spectra before and after annealing do not show significant differences. The addition of TWEEN 20 detergent in solution has no influence on the shape of differential spectra for all analyzed samples.

4. Discussion

The first result of this study is the identification of a specific CpG island at *IMOOD* promoter containing a CpG site (CpG site 2) differentially methylated in DNA obtained from PBMCs of OCD subjects when compared to genomic material collected from healthy controls. This alteration was significantly correlated with the increased expression of the gene that we previously reported (Piras et al., 2020). It has already been observed that epigenetic alterations appear to be relevant in different pathologies (Tafani et al., 2020) including OCD (D'Addario et al., 2022a, 2022b; Schiele et al., 2022). So far, studies into the peripheral DNA methylation signatures in OCD have mostly focused on candidate-genes (Endres et al., 2022).

Our data on *IMOOD* DNA methylation add a new piece in the puzzle and we thus propose the involvement of its transcriptional regulation in OCD suggesting a role for CpG methylation at gene promoter. A recent meta-analysis study reported differential methylation in opioid users when compared to nonusers at CpGs annotated to 6 genes, among these *IMOOD* gene (Lee et al., 2023). It is of interest to note that the level of compulsivity and obsessionality in opioid dependence has been found to be comparable to that found in OCD (Friedman et al., 2000).

In order to deeply analyze the molecular mechanisms behind *IMOOD* regulation, we performed a bioinformatic analysis and we noticed that *IMOOD* promoter has a quite extended region with a peculiar characteristic: a remarkable high percentage of guanines. This guanine-rich sequence also includes CpG site 2. These two concomitant elements caught our attention, letting us hypothesize that different regulators of gene expression could be involved.

Considering that *KIT* gene promoter, with a well-known and characterised G4-forming region accounts for a lower percentage of G, with respect to *IMOOD* (about 37% vs 50%), we focused on the possibility that *IMOOD* promoter could form G-quadruplexes (G4s).

G4s are DNA secondary structures consisting of stacks of planar G-tetrads, which are preferentially stabilized by monovalent

Table 4
Competition assay curves fitting parameters.

OLIGO	bKIT2			bImood			b2stackG4
competitor	KIT2	KIT2 meth	KIT2 mut	Imood	Imood meth	Imood mut	Imood (displacement)
HillSlope	−0.8987	−0.9813	−0.6714	−1.533	−1.405	0.3033	−1.473
IC50 (M)	3.37E-07	2.26E-07	1.50E-05	2.59E-07	2.74E-07	6.62E-20	1.08E-08
R squared	0.9813	0.993	0.8084	0.9962	0.999	0.2605	0.9965

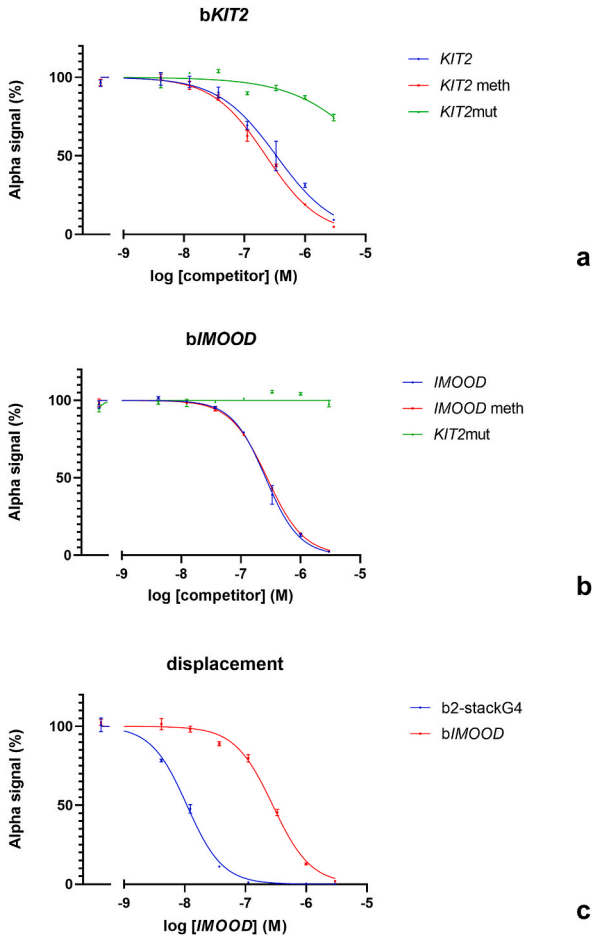

Fig. 2. a, b. Alpha competition assays for the determination of the constant affinity K_d of G4s vs the monoclonal AbG4 antibody. Competitors to the binding of b-consensus oligos (**a**. bKIT2; **b**. bIMOOD) to AbG4 are respectively the untagged oligo before (cyan) and after (red) full enzymatic methylation. Untagged non-specific mutated KIT2 oligo (green) was used in both cases as negative control. Panel **c**: Alpha displacement assay of biotinylated 2-stack predicted G4 oligo (blue) using as a competitor the untagged IMOOD G4 sequence gives a calculated IC50 value much lower (1 order of magnitude) with respect to bIMOOD (red), addressing to a very low affinity for the AbG4 antibody (see Table 4 for fitting values).

cations (the strongest is K^+) centrally coordinated to the O6 atoms of guanines (Spiegel et al., 2020).

G4 formation can be predicted *in silico*, using computational algorithms based on the search of a G-rich motif (Puig Lombardi and Londoño-Vallejo, 2020) and this approach allowed to predict the presence of at least one G4 motif in >40% human gene promoters (Huppert and Balasubramanian, 2007).

Recent evidence suggests that G4s are involved in key genome functions such as transcription, replication, genome stability, and epigenetic regulation (Spiegel et al., 2020). In particular, G4s have recently been shown to be target binding sites for a large number of transcription factors (TFs) when located at gene promoters (Fang et al., 2022; Spiegel et al., 2020). Moreover, it has been demonstrated that G4s can influence methylation at CpG islands (Fang et al., 2022; Mao et al., 2018) and appear to be prevalent TF binding hubs in human chromatin (Spiegel et al., 2021), in particular for highly expressed genes and their binding can be affected by cytosine methylation (Patel et al., 2020; Yin et al., 2017).

We already successfully utilized the Alpha technology to propose an innovative assay to measure the interaction of DNA motifs to TFs and quantitatively evaluate the effect of CpG methylation on binding affinity (Sabatucci et al., 2020). Here, the use of Alpha method allowed us not only to verify the formation of G4 structures on *IMOOD* and on positive and negative control sequences, but also to verify the structural effect of CpG methylation on G4 stability. Moreover, the high sensitivity of the method allowed us to verify the difference in affinity for the monoclonal AbG4 for 4-stack stable G4s vs a predicted low-score 2-stack G4.

In our experimental conditions, CpG methylation, for both *KIT* and *IMOOD*, does not substantially affect the G4 structure. Indeed, CpG methylation has been shown to have structural effects on G4 stability, stabilizing some G4 structures and destabilizing some others. G4 sequences occur more frequently at gene promoters, thus also in CpG islands (Huppert and Balasubramanian, 2007; Zhao et al., 2007) and have been associated to suppression as well as activation of the transcription (Stevens et al., 2022).

At the level of gene promoters, CpG methylation has been suggested to act as an epigenetic transcription regulator, as this

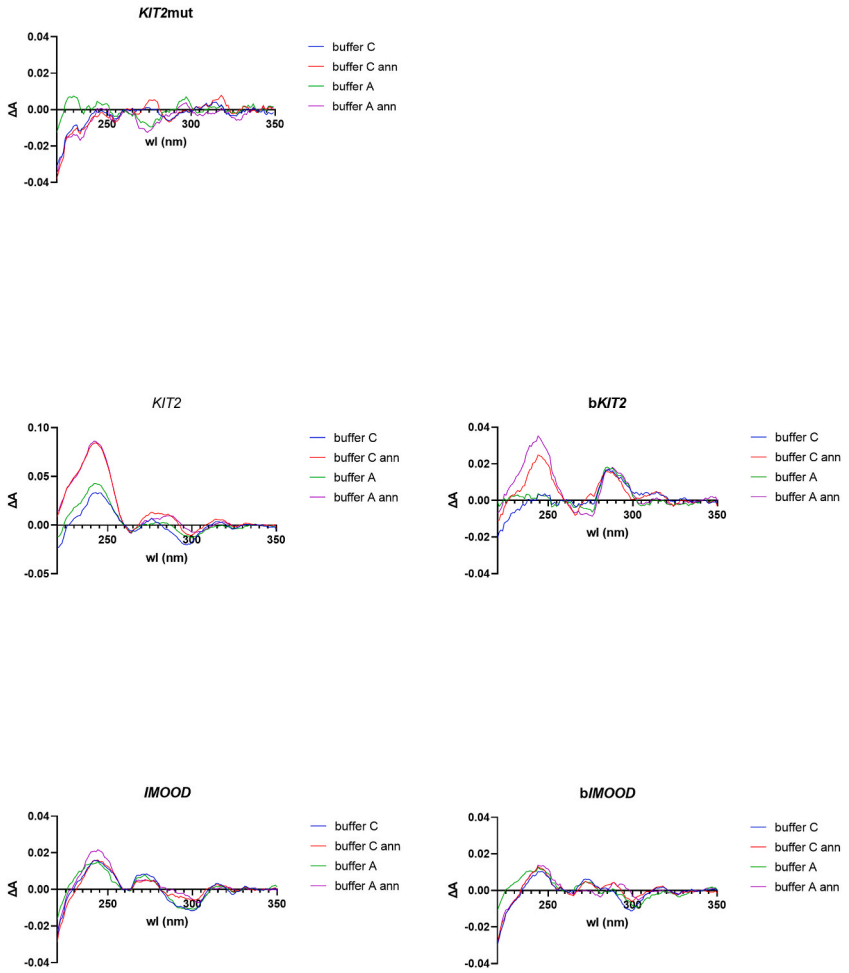

Fig. 3. Differential UV spectra. Left panel: wt oligos. Right panel: biotinylated oligos. The normalized spectra of all samples measured in Buffer D (Tris/HCl 10 mM, pH 7.4) were subtracted to the ones in Buffer C (Tris 10 mM pH 7.4 KCl 100 mM); or Buffer A (Tris 10 mM pH 7.4, KCl 100 mM, Tween20 0.1% v/v) before or after annealing (ann).

epigenetic modification can affect the binding activity of G4-binding proteins, including TFs (Tsukakoshi et al., 2018), and this could actually be the mechanism occurring at *IMOOD* promoter. Moreover, a recent bioinformatic study hypothesized that G4 structures may act as epigenetic regulatory elements potentially able to recruit enzymes adding or removing methylation marks suggesting that G4 formation might generally evoke DNA-methylation perturbation not necessarily promoting hyper- or hypomethylation (Rauchhaus et al., 2022).

Our data overall support the hypothesis that *IMOOD* expression is modulated by DNA methylation in OCD. This modification targets a specific CpG site in *IMOOD* promoter and a significant difference has been reported between OCD and healthy subjects.

At the same time, *IMOOD* promoter can fold in multiple G-quadruplex structures, and we verified experimentally that the observed CpG motif differently methylated is constitutive of a G4 structure and does not affect its stability in the presence of K^+ ions in solution.

Our *in-silico* analysis suggests that the reported one could be one of several points where CpG motifs are constitutive of G4 structures, and thus that the interplay between CpG methylation and G4s could be a crucial regulation mechanism for *IMOOD* expression.

It would be thus possible that *IMOOD* promoter is silenced in homeostatic conditions due to higher levels of DNA methylation, whereas it becomes more accessible to TFs in pathological conditions, such as in OCD, inducing an increase in its expression. Further biomolecular studies will be of help to deepen our knowledge on the role and regulation of this gene and to characterize the binding of the different TFs. The data we report on the epigenetic and on the DNA conformations at specific genomic sequences could represent a novel approach to better characterize important biological functions, such as the regulation of gene expression, altered nucleosome positioning (stable G4s induce subsequent genomic rearrangements), or even the control of genomic imprinting.

In conclusion, our data could be of relevance in order not only to suggest new biomarkers and thus new targets but also new therapeutic approaches for OCD, as well as other disorders where these kinds of alterations might occur. For instance, it might be not so unlikely to prospect in those with known altered IMOOD gene regulation, methyl donor supplementation that might be functional in

reduce *IMOOD* up-regulation by modifying TFs recruiting on G4 motifs.

Intellectual property

We confirm that we have given due consideration to the protection of intellectual property associated with this work and that there are no impediments to publication, including the timing of publication, with respect to intellectual property. In so doing we confirm that we have followed the regulations of our institutions concerning intellectual property.

Funding

This research was funded by the European Union – Next Generation EU. Project Code: ECS00000041; Project CUP: C43C22000380007; Project Title: Innovation, digitalization and sustainability for the diffused economy in Central Italy – VITALITY.

Research ethics

We further confirm that any aspect of the work covered in this manuscript that has involved human patients has been conducted with the ethical approval of all relevant bodies and that such approvals are acknowledged within the manuscript.

Authorship

We confirm that the manuscript has been read and approved by all named authors.
We confirm that the order of authors listed in the manuscript has been approved by all named authors.

Declaration of competing interest

We wish to confirm that there are no known conflicts of interest associated with this publication and there has been no significant financial support for this work that could have influenced its outcome.

Data availability

Data will be made available on request.

Acknowledgment

This research was funded by the European Union – Next Generation EU. Project Code: ECS00000041; Project CUP: C43C22000380007; Project Title: Innovation, digitalization and sustainability for the diffused economy in Central Italy – VITALITY.

Appendix A. Supplementary data

Supplementary data to this article can be found online at https://doi.org/10.1016/j.jbior.2023.100976.

References

American Psychiatric Association, 2013. DSM-5 diagnostic classification. Diagn. Stat. Manual Mental. Disord.

Biffi, G., Tannahill, D., McCafferty, J., Balasubramanian, S., 2013. Quantitative visualization of DNA G-quadruplex structures in human cells. Nat. Chem. 5, 182–186. https://doi.org/10.1038/nchem.1548.

Crocco, P., Montesanto, A., Passarino, G., Rose, G., 2016. Polymorphisms falling within putative miRNA target sites in the 3′UTR region of SIRT2 and DRD2 genes are correlated with human longevity. J. Gerontol. - Series Biol.l Sci. Med.Sci. 71, 586–592. https://doi.org/10.1093/gerona/glv058.

D'Addario, C., Bellia, F., Benatti, B., Grancini, B., Vismara, M., Pucci, M., De Carlo, V., Viganò, C., Galimberti, D., Fenoglio, C., Scarpini, E., Maccarrone, M., Dell'Osso, B., 2019. Exploring the role of BDNF DNA methylation and hydroxymethylation in patients with obsessive compulsive disorder. J. Psychiatr. Res. 114, 17–23. https://doi.org/10.1016/j.jpsychires.2019.04.006.

D'Addario, C., Macellaro, M., Bellia, F., Benatti, B., Annunzi, E., Palumbo, R., Conti, D., Fasciana, F., Vismara, M., Varinelli, A., Ferrara, L., Celebre, L., Viganò, C., Dell'Osso, B., 2022a. In search for biomarkers in obsessive-compulsive disorder: new evidence on saliva as a practical source of DNA to assess epigenetic regulation. Curr. Med. Chem. 29, 5782–5791. https://doi.org/10.2174/0929867328666211208115536.

D'Addario, C., Pucci, M., Bellia, F., Girella, A., Sabatucci, A., Fanti, F., Vismara, M., Benatti, B., Ferrara, L., Fasciana, F., Celebre, L., Viganò, C., Elli, L., Sergi, M., Maccarrone, M., Buzzelli, V., Trezza, V., Dell'Osso, B., 2022b. Regulation of oxytocin receptor gene expression in obsessive–compulsive disorder: a possible role for the microbiota-host epigenetic axis. Clin. Epigenet. 14, 47. https://doi.org/10.1186/s13148-022-01264-0.

De Bruijn, C., Beun, S., Graaf, R. De, Have, M. Ten, Denys, D., 2010. Subthreshold symptoms and obsessive-compulsive disorder: evaluating the diagnostic threshold. Psychol. Med. 40, 989–997. https://doi.org/10.1017/S0033291709991012.

Dell'Osso, B., Altamura, A.C., Mundo, E., Marazziti, D., Hollander, E., 2007. Diagnosis and treatment of obsessive-compulsive disorder and related disorders. Int. J. Clin. Pract. https://doi.org/10.1111/j.1742-1241.2006.01167.x.

Ducani, C., Bernardinelli, G., Högberg, B., Keppler, B.K., Terenzi, A., 2019. Interplay of three G-quadruplex units in the KIT promoter. J. Am. Chem. Soc. 141, 10205–10213. https://doi.org/10.1021/jacs.8b12753.

Endres, D., Hannibal, L., Zaltenbach, B., Schiele, M.A., Runge, K., Nickel, K., Berger, B., Domschke, K., Venhoff, N., Prüss, H., Tebartz van Elst, L., 2022. Case Report: possible autoimmune obsessive-compulsive disorder with postpartum onset. Front. Immunol. 13, 970448 https://doi.org/10.3389/fimmu.2022.970448.
Fang, S., Liu, S., Yang, D., Yang, L., Hu, C.D., Wan, J., 2022. Decoding regulatory associations of G-quadruplex with epigenetic and transcriptomic functional components. Front. Genet. 13, 957023 https://doi.org/10.3389/fgene.2022.957023.
Farré, D., Roset, R., Huerta, M., Adsuara, J.E., Roselló, L., Albà, M.M., Messeguer, X., 2003. Identification of patterns in biological sequences at the ALGGEN server: PROMO and MALGEN. Nucleic Acids Res. 31, 3651–3653. https://doi.org/10.1093/nar/gkg605.
Faul, F., Erdfelder, E., Lang, A.-G., Buchner, A., 2007. G*Power 3: a flexible statistical power analysis program for the social, behavioral, and biomedical sciences. Behav. Res. Methods 39, 175–191. https://doi.org/10.3758/BF03193146.
First, M.B., Reed, G.M., Hyman, S.E., Saxena, S., 2015. The development of the ICD-11 clinical descriptions and diagnostic guidelines for mental and behavioural disorders. World Psychiatr. 14, 82–90. https://doi.org/10.1002/wps.20189.
Fontenelle, I.S., Fontenelle, L.F., Borges, M.C., Prazeres, A.M., Rangé, B.P., Mendlowicz, M.V., Versiani, M., 2010. Quality of life and symptom dimensions of patients with obsessive–compulsive disorder. Psychiatr. Res. 179, 198–203. https://doi.org/10.1016/J.PSYCHRES.2009.04.005.
Friedman, I., Dar, R., Shilony, E., 2000. Compulsivity and obsessionality in opioid addiction. J. Nerv. Ment. Dis. 188, 155–162.
García-Soriano, G., Rufer, M., Delsignore, A., Weidt, S., 2014. Factors associated with non-treatment or delayed treatment seeking in OCD sufferers: a review of the literature. Psychiatr. Res. 220, 1–10. https://doi.org/10.1016/J.PSYCHRES.2014.07.009.
Goodman, W.K., Price, L.H., Rasmussen, S.A., Mazure, C., Fleischmann, R.L., Hill, C.L., Heninger, G.R., Charney, D.S., 1989. The Yale-Brown obsessive compulsive scale: I. Development, use, and reliability. Arch. Gen. Psychiatr. 46, 1006–1011. https://doi.org/10.1001/archpsyc.1989.01810110048007.
Gray, R.D., Chaires, J.B., 2012. Isothermal folding of G-quadruplexes. Methods 57, 47–55. https://doi.org/10.1016/j.ymeth.2012.04.006.
Hänsel-Hertsch, R., Beraldi, D., Lensing, S.V., Marsico, G., Zyner, K., Parry, A., Di Antonio, M., Pike, J., Kimura, H., Narita, M., Tannahill, D., Balasubramanian, S., 2016. G-quadruplex structures mark human regulatory chromatin. Nat. Genet. 48, 1267–1272. https://doi.org/10.1038/ng.3662.
Harich, B., Klein, M., Ockeloen, C.W., van der Voet, M., Schimmel-Naber, M., de Leeuw, N., Schenck, A., Franke, B., 2020. From man to fly – convergent evidence links FBXO25 to ADHD and comorbid psychiatric phenotypes. JCPP (J. Child Psychol. Psychiatry) 61, 545–555. https://doi.org/10.1111/jcpp.13161.
Hashimoto, H., Olanrewaju, Y.O., Zheng, Y., Wilson, G.G., Zhang, X., Cheng, X., 2014. Wilms tumor protein recognizes 5-carboxylcytosine within a specific DNA sequence. Genes Dev. 28, 2304–2313. https://doi.org/10.1101/gad.250746.114.
Huppert, J.L., Balasubramanian, S., 2007. G-quadruplexes in promoters throughout the human genome. Nucleic Acids Res. 35, 406–413. https://doi.org/10.1093/nar/gkl1057.
Karsisiotis, A.I., Hessari, N.M.A., Novellino, E., Spada, G.P., Randazzo, A., Webba Da Silva, M., 2011. Topological characterization of nucleic acid G-quadruplexes by UV absorption and circular dichroism. Angew. Chem. Int. Ed. 50, 10645–10648. https://doi.org/10.1002/anie.201105193.
Kikin, O., D'Antonio, L., Bagga, P.S., 2006. QGRS Mapper: a web-based server for predicting G-quadruplexes in nucleotide sequences. Nucleic Acids Res. 34, w676–w682. https://doi.org/10.1093/nar/gkl253.
Koran, L.M., Simpson, H.B., 2013. Guideline Watch (March 2013): Practice Guideline for the Treatment of Patients with Obsessive-Compulsive Disorder. APA Practice Guidelines.
Korec, E., Ungrová, L., Hejnar, J., Grieblová, A., 2022. Four novel genes associated with longevity found in Cane corso purebred dogs. BMC Vet. Res. 18, 188. https://doi.org/10.1186/s12917-022-03290-9.
Kuersten, S., Goodwin, E.B., 2003. The power of the 3′ UTR: translational control and development. Nat. Rev. Genet. https://doi.org/10.1038/nrg1125.
Laddachote, S., Ishii, R., Yoshida, W., 2021. Effects of CpG methylation on the thermal stability of c-kit2, c-kit*, and c-kit1 G-quadruplex structures. BBA Adv. 1, 100007 https://doi.org/10.1016/j.bbadva.2021.100007.
Lee, M., Joehanes, R., McCartney, D.L., Kho, M., Hüls, A., Wyss, A.B., Liu, C., Walker, R.M., R Kardia, S.L., Wingo, T.S., Burkholder, A., Ma, J., Campbell, A., Wingo, A. P., Huan, T., Sikdar, S., Keshawarz, A., Bennett, D.A., Smith, J.A., Evans, K.L., Levy, D., London, S.J., 2023. Opioid medication use and blood DNA methylation: epigenome-wide association meta-analysis. Epigenomics 1479–1492. https://doi.org/10.2217/epi-2022-0353.
Levy, H.C., McLean, C.P., Yadin, E., Foa, E.B., 2013. Characteristics of individuals seeking treatment for obsessive-compulsive disorder. Behav. Ther. 44, 408–416. https://doi.org/10.1016/J.BETH.2013.03.007.
Li, L.-C., Dahiya, R., 2002. MethPrimer: designing primers for methylation PCRs. Bioinformatics.
Mao, S.Q., Ghanbarian, A.T., Spiegel, J., Martínez Cuesta, S., Beraldi, D., Di Antonio, M., Marsico, G., Hänsel-Hertsch, R., Tannahill, D., Balasubramanian, S., 2018. DNA G-quadruplex structures mold the DNA methylome. Nat. Struct. Mol. Biol. 25, 951–957. https://doi.org/10.1038/s41594-018-0131-8.
Maxwell, J.A.J., Maxwell, 2013. A Model for qualitative research design. Qualitative Research Design: An Interactive Approach 62.
Messeguer, X., Escudero, R., Farré, D., Núñez, O., Martínez, J., Albà, M.M., 2002. PROMO: detection of known transcription regulatory elements using species-tailored searches. Bioinformatics 18, 333–334. https://doi.org/10.1093/bioinformatics/18.2.333.
Morimoto, Y., Ono, S., Imamura, A., Okazaki, Y., Kinoshita, A., Mishima, H., Nakane, H., Ozawa, H., Yoshiura, K.I., Kurotaki, N., 2017. Deep sequencing reveals variations in somatic cell mosaic mutations between monozygotic twins with discordant psychiatric disease. Hum. Genome Var. 4, 17032 https://doi.org/10.1038/hgv.2017.32.
Patel, M., Patel, D., Datta, S., Singh, U., 2020. CGGBP1-regulated cytosine methylation at CTCF-binding motifs resists stochasticity. BMC Genet. 21, 84. https://doi.org/10.1186/s12863-020-00894-8.
Peterková, K., Durník, I., Marek, R., Plavec, J., Podbevšek, P., 2021. C-kit2 G-quadruplex stabilized via a covalent probe: exploring G-quartet asymmetry. Nucleic Acids Res. 49, 8947–8960. https://doi.org/10.1093/nar/gkab659.
Piras, G., Rattazzi, L., Paschalidis, N., Oggero, S., Berti, G., Ono, M., Bellia, F., D'Addario, C., Dell'Osso, B., Pariante, C.M., Perretti, M., D'Acquisto, F., 2020. Immunomodulin: a new anxiogenic factor produced by Annexin-A1 transgenic autoimmune-prone T cells. Brain Behav. Immun. 87, 689–702. https://doi.org/10.1016/J.BBI.2020.02.015.
Pucci, M., Bonaventura, M.V.M. Di, Vezzoli, V., Zaplatic, E., Massimini, M., Mai, S., Sartorio, A., Scacchi, M., Persani, L., Maccarrone, M., Cifani, C., D'Addario, C., 2019. Preclinical and clinical evidence for a distinct regulation of mu opioid and type 1 cannabinoid receptor genes expression in obesity. Front. Genet. 10, 523. https://doi.org/10.3389/fgene.2019.00523.
Puig Lombardi, E., Londoño-Vallejo, A., 2020. A guide to computational methods for G-quadruplex prediction. Nucleic Acids Res. https://doi.org/10.1093/nar/gkz1097.
Rauchhaus, J., Robinson, J., Monti, L., Di Antonio, M., 2022. G-Quadruplexes mark sites of methylation instability associated with ageing and cancer. Genes 13, 1665. https://doi.org/10.3390/genes13091665.
Sabatucci, A., Berchet, V., Bellia, F., Maccarrone, M., Dainese, E., D'Addario, C., Pucci, M., 2020. A new methodological approach for in vitro determination of the role of DNA methylation on transcription factor binding using AlphaScreen® analysis: focus on CREB1 binding at hBDNF promoter IV. J. Neurosci. Methods. https://doi.org/10.1016/j.jneumeth.2020.108720.
Schiele, M.A., Lipovsek, J., Schlosser, P., Soutschek, M., Schratt, G., Zaudig, M., Berberich, G., Köttgen, A., Domschke, K., 2022. Epigenome-wide DNA methylation in obsessive-compulsive disorder. Transl. Psychiatry 12, 221. https://doi.org/10.1038/s41398-022-01996-w.
Spiegel, J., Adhikari, S., Balasubramanian, S., 2020. The structure and function of DNA G-quadruplexes. Trends Chem. https://doi.org/10.1016/j.trechm.2019.07.002.
Spiegel, J., Cuesta, S.M., Adhikari, S., Hänsel-Hertsch, R., Tannahill, D., Balasubramanian, S., 2021. G-quadruplexes are transcription factor binding hubs in human chromatin. Genome Biol. 22, 117. https://doi.org/10.1186/s13059-021-02324-z.
Stevens, A.J., de Jong, L., Kennedy, M.A., 2022. The dynamic regulation of G-quadruplex DNA structures by cytosine methylation. Int. J. Mol. Sci. https://doi.org/10.3390/ijms23052407.
Tafani, X., Pascale, E., Fattapposta, F., Pucci, M., D'Addario, C., Adriani, W., 2020. Cross-correlations between motifs in the 5′-UTR of DAT1 gene: findings from Parkinson's disease. Adv. Biol. Regul. 78, 100753 https://doi.org/10.1016/j.jbior.2020.100753.

Tsukakoshi, K., Saito, S., Yoshida, W., Goto, S., Ikebukuro, K., 2018. CpG methylation changes G-Quadruplex structures derived from gene promoters and interaction with VEGF and SP1. Molecules 23, 944. https://doi.org/10.3390/molecules23040944.

Yin, Y., Morgunova, E., Jolma, A., Kaasinen, E., Sahu, B., Khund-Sayeed, S., Das, P.K., Kivioja, T., Dave, K., Zhong, F., Nitta, K.R., Taipale, M., Popov, A., Ginno, P.A., Domcke, S., Yan, J., Schübeler, D., Vinson, C., Taipale, J., 2017. Impact of cytosine methylation on DNA binding specificities of human transcription factors. Science 1979 (356), eaaj2239. https://doi.org/10.1126/science.aaj2239.

Zhao, Y., Du, Z., Li, N., 2007. Extensive selection for the enrichment of G4 DNA motifs in transcriptional regulatory regions of warm blooded animals. FEBS Lett. 581, 1951–1956. https://doi.org/10.1016/j.febslet.2007.04.017.